Resonances contribution to two-photon exchange effects and possible large forward-backward asymmetry in $e^+e^- \leftrightarrow p\bar{p}$

Hai-Qing Zhou [1,3*], Bing-Song Zou [2,3]

[1] Department of Physics, Southeast University, Nanjing 211189, P. R. China
[2] Institute of High Energy Physics, CAS, Beijing 100049, P. R. China
[3] Theoretical Physics Center for Science Facilities, CAS, Beijing 100049, P. R. China

Abstract

The resonances $(\eta_c, \chi_{c0,c2})$ contribution to two-photon exchange (TPE) effects in $e^+e^- \leftrightarrow p\bar{p}$ is calculated in a simple hadronic model. The calculation shows the TPE contributions by resonance χ_{c2}, which are dependent on the unknown phases $\phi_{E,M}$ of proton's time-like form factors $G_{E,M}$, are much larger than the TPE contributions by non-resonance and are comparable with measurement precision of coming PANDA detector at $\sqrt{s} \sim M_{\chi_{c2}}$ for most $\phi_{E,M}$.

PACS numbers: 13.40.Gp, 13.60.-r, 25.30.-c.
Key words: resonance, two-photon exchange, proton, form factor

1 Introduction

The structure of nucleon is one of the most important topics in the hadronic physics. The electromagnetic interaction provides a clean method to measure such a structure. One of the most important measurement is to determine the electromagnetic form factors $G_E(Q^2)$ and $G_M(Q^2)$ of nucleon. The measurements of $R = \mu_p G_E(Q^2)/G_M(Q^2)$ at space-like region by polarized method and Roesenbluth method [1] indicate it is not trivial to extract the form factors directly from the angle dependence of cross section. Since then, the two-photon exchange (TPE) effects attract many interest. In the literature, the TPE contributions in $ep \to ep$ and $e^+e^- \leftrightarrow p\bar{p}$ have been estimated by some model dependent methods [2–7] and model independent analysis [8–13] (see recent review articles [14]). Experimentally, to detect the TPE effects directly, the measurements of $R_{e^+e^-}$ defined as the ratio of e^+p to e^-p differential cross sections are proposed by VEPP-3 [15], JLab [16] and OLYMPUS [17], and the measurement of forward-backward asymmetry in $p\bar{p} \to e^+e^-$ is proposed by PANDA [18]. In this work, we estimate the TPE contributions in the unpolarized processes $e^+e^- \leftrightarrow p\bar{p}$ when $\sqrt{s}$ lies in the resonances $\eta_c, \chi_{c0,c2}$ region. We arrange our discussion as follows: in Section 2, we review the contributions of vector resonances (ψ, ψ') in $e^+e^- \to p\bar{p}$ by one-photon exchange (OPE); in Section 3, we discuss the TPE contributions by $\eta_c, \chi_{c0,c2}$ and in Section 4 we present the numerical results and give a discussion.

2 Resonances contribution in $e^+e^- \to p\bar{p}$ by OPE

Considering the process $e^+(k_2) + e^-(k_1) \to p(p_2) + \bar{p}(p_1)$ at tree level, by the vector-meson-dominance model, the 1^{--} resonances contributions can be described by diagrams in the left panel of Fig.1, where we limit our discussion in the charmonium region. The couplings of 1^{--} charmonium ψ, ψ' with $p\bar{p}$ are

*E-mail: zhouhq@mail.ihep.ac.cn

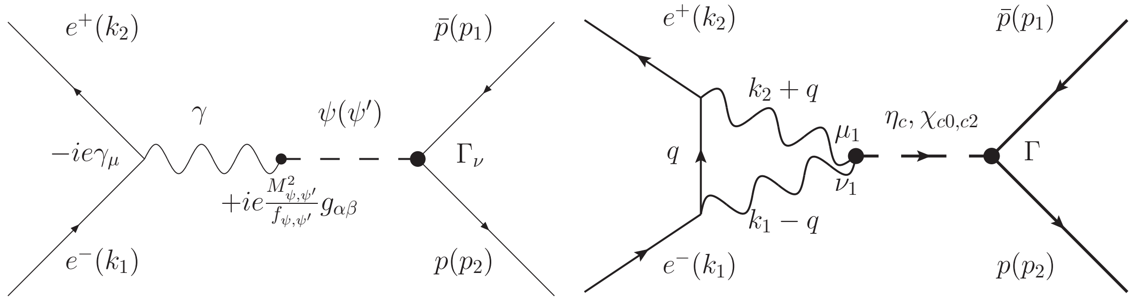

Figure 1: Left panel: diagrams for 1^{--} resonances (ψ,ψ') contributions in $e^+e^- \to p\bar{p}$ by one photon annihilation; right panel: diagrams for $0^{-+}, 0^{++}, 2^{++}$ resonances ($\eta_c, \chi_{c0,c2}$) contributions in $e^+e^- \to p\bar{p}$ by two photon annihilating.

described as in Ref. [19] with a little different notation

$$\Gamma_\nu^{(\psi p\bar{p},\psi' p\bar{p})} = -i(g_{\psi,\psi'}\gamma_\nu + \frac{i\kappa_{\psi,\psi'}}{2M_N}\sigma_{\nu\rho}q^\rho), \tag{1}$$

where $M_N = 0.938$ GeV is the mass of proton, $q = (\sqrt{s}, 0, 0, 0)$ in the c.m. frame [20]. By these Born diagrams, the unpolarized differential cross section in the c.m. frame can be written as

$$\begin{aligned}\frac{d\sigma^0}{d\Omega} \quad = \quad & \frac{\alpha_{em}^2 M_\psi^4 (1-4M_N^2/s)^{1/2}}{4s^2}\frac{[4M_N^2|G_E^\psi|^2(1-\cos^2\theta)+s|G_M^\psi|^2(1+\cos^2\theta)]}{f_\psi^2((s-M_\psi^2)^2+\Gamma_\psi^2 M_\psi^2)} + \\ & \frac{\alpha_{em}^2 M_{\psi'}^4 (1-4M_N^2/s)^{1/2}}{4s^2}\frac{[4M_N^2|G_E^{\psi'}|^2(1-\cos^2\theta)+s|G_M^{\psi'}|^2(1+\cos^2\theta)]}{f_{\psi'}^2((s-M_{\psi'}^2)^2+\Gamma_{\psi'}^2 M_{\psi'}^2)} + \\ & \frac{\alpha_{em}^2 M_\psi^2 M_{\psi'}^2 (1-4M_N^2/s)^{1/2}}{4s^2} 2Re\{\frac{4M_N^2 G_E^\psi G_E^{\psi'*}(1-\cos^2\theta)+sG_M^\psi G_M^{\psi'*}(1+\cos^2\theta)}{f_\psi f_{\psi'}^*(s-M_\psi^2+i\Gamma_\psi M_\psi)(s-M_{\psi'}^2-i\Gamma_{\psi'}M_{\psi'})}\}, \end{aligned} \tag{2}$$

with $M_\psi = 3.096$ GeV, $M'_\psi = 3.686$ GeV the masses of ψ, ψ', θ the scattering angle in the c.m. frame, and $G_E^{\psi,\psi'} = g_{\psi,\psi'} + \kappa_{\psi,\psi'}s/4M_N^2$, $\;G_M^{\psi,\psi'} = g_{\psi,\psi'} + \kappa_{\psi,\psi'}$. Since we limit the discussion in the charmonium region, it is a good approximation to treat the couplings $f_{\psi,\psi'}, G_{E,M}^{\psi,\psi'}$ as constants which are constrained by [19]

$$\begin{aligned}\Gamma_{\psi,\psi'\to p\bar{p}} &= \frac{(1-4M_N^2/M_{\psi,psi'}^2)^{1/2}}{12\pi M_{\psi,\psi'}}(2M_N^2|G_E^{\psi,\psi'}|^2 + M_{\psi,\psi'}^2|G_M^{\psi,\psi'}|^2), \\ \Gamma_{\psi,\psi'\to e^+e^-} &= \frac{4\pi\alpha_{em}^2 M_{\psi,\psi'}}{3f_{\psi,\psi'}^2}, \qquad \alpha_{\psi,\psi'} = \frac{1-4M_N^2/s|G_E^{\psi,\psi'}/G_M^{\psi,\psi'}|^2}{1+4M_N^2/s|G_E^{\psi,\psi'}/G_M^{\psi,\psi'}|^2},\end{aligned} \tag{3}$$

with $\alpha_{\psi,\psi'} \approx 0.67$ at corresponding $\sqrt{s} = M_{\psi,\psi'}$. In the following calculation, for simplicity, we naively assume that the phases of G_E^ψ and $G_E^{\psi'}$, G_M^ψ and $G_M^{\psi'}$ are the same, respectively. By these assumptions and the constraint conditions, only two physical parameters $\phi_{M,E}$ which are defined as $G_{E,M}^{\psi,\psi'} = e^{i\phi_{E,M}}|G_{E,M}^{\psi,\psi'}|$ are left as unknown.

3 Resonances contribution in $e^+e^- \to p\bar{p}$ by TPE

When considering the TPE contributions from other resonances in charmonium region, the diagrams shown in the right panel of Fig.1 should be considered, where only $0^{-+}, 0^{++}, 2^{++}$ resonances are included

since their couplings to $p\bar{p}$ and 2γ are relatively large. The couplings of $0^{-+}, 0^{++}, 2^{++}$ charmonium with two-photon can be described as in [21],

$$
\begin{aligned}
\Gamma^{\mu_1\nu_1}_{\gamma\gamma\eta_c} &= -ig_{\eta_c\gamma\gamma}D\varepsilon^{\mu_1\mu_2\nu_1\nu_2}(k_2+q)_{\mu_2}(k_1-q)_{\nu_2},\\
\Gamma^{\mu_1\nu_1}_{\gamma\gamma\chi_{c0}} &= -ig_{\chi_{c0}\gamma\gamma}D^2\{[(k_1-q)\cdot(k_2+q)g^{\mu_1\nu_1}-(k_1-q)^{\mu_1}(k_2+q)^{\nu_1}][M^2_{\chi_{c0}}+(k_1-q)\cdot(k_2+q)]\\
&\quad +(k_2+q)^{\mu_1}(k_2+q)^{\nu_1}(k_1-q)^2+(k_1-q)^{\mu_1}(k_1-q)^{\nu_1}(k_2+q)^2\\
&\quad -(k_1-q)^2(k_2+q)^2g^{\mu_1\nu_1}-(k_2+q)^{\nu_1}(k_1-q)^{\mu_1}(k_1-q)\cdot(k_2+q)\},\\
\Gamma^{\mu_1\nu_1;\mu_2\nu_2}_{\gamma\gamma\chi_{c2}} &= -ig_{\chi_{c2}\gamma\gamma}D^2\{g^{\mu_1\mu_2}g^{\nu_1\nu_2}(k_1-q)\cdot(k_2+q)-g^{\mu_1\nu_1}(k_1-q)^{\mu_2}(k_2+q)^{\nu_2}\\
&\quad -(k_2+q)^{\nu_1}(k_1-q)^{\mu_2}g^{\mu_1\nu_2}-(k_1-q)^{\mu_1}(k_2+q)^{\mu_2}g^{\nu_1\nu_2}\},
\end{aligned}
\tag{4}
$$

where k_1-q, k_2+q are the momentums of photons, μ_1, ν_1 are the corresponding Lorentz indexes and $D=[(q+k_2/2-k_1/2)^2-m_c^2+i\epsilon]^{-1}$ with m_c the mass of c quark, and we take $m_c = 1.5$ GeV in the following calculation.

For the couplings of $0^{-+}, 0^{++}, 2^{++}$ charmonium with $p\overline{p}$, for simplicity we take them the same as those with e^+e^-, which can be described as in [21],

$$
\begin{aligned}
\Gamma_{\eta_c p\bar{p}} &= g_{\eta_c p\bar{p}}\gamma_5,\\
\Gamma_{\chi_{c0} p\bar{p}} &= g_{\chi_{c0} p\bar{p}},\\
\Gamma^{\mu\nu}_{\chi_{c2} p\bar{p}} &= g_{\chi_{c2} p\bar{p}}(p_1-p_2)^\nu\gamma^\mu.
\end{aligned}
\tag{5}
$$

These couplings are constrained by the physical decay width $\Gamma(\eta_c, \chi_{c0,c2} \to \gamma\gamma, p\bar{p})$ with

$$
\begin{aligned}
\Gamma_{\chi_{c2}\to\gamma\gamma} &= \frac{g^2_{\gamma\gamma\chi_{c2}}M^3_{\chi_{c2}}}{15(4m_c^2+M^2_{\chi_2})^2\pi},\\
\Gamma_{\chi_{c2}\to p\bar{p}} &= \frac{g^2_{\chi_{c2}p\bar{p}}\sqrt{M^2_{\chi_{c2}}-4M_N^2}(3M^4_{\chi_{c2}}-4M^2_{\chi_{c2}}M_N^2-32M_N^4)}{120\pi M^2_{\chi_{c2}}},
\end{aligned}
\tag{6}
$$

where $M_{\chi_2} = 3.556$ GeV is the mass of χ_{c2}, $\Gamma_{\chi_{c2}\to\gamma\gamma} = 1.97$ MeV $\times(2.56\times10^{-4}) = 5.04\times10^{-4}$ MeV and $\Gamma_{\chi_{c2}\to p\bar{p}} = 1.97$ MeV $\times(7.2\times10^{-5}) = 1.42\times10^{-4}$ MeV [22]. This results in

$$
|g_{\gamma\gamma\chi_{c2}}| = 1.57\times10^{-2}, |g_{\chi_{c2}p\bar{p}}| = 7.39\times10^{-4}. \tag{7}
$$

Here, only $g_{\chi_{c2}p\bar{p}}$ and $g_{\gamma\gamma\chi_{c2}}$ are given since the calculation shows the contributions from η_c and χ_{c0} are identically zero because of the Dirac structure of corresponding unpolarized differential cross sections. For simplicity, we assume the phases of these two couplings are zero.

The propagator of χ_{c2} is described as the standard Breit-Wigner form [23]

$$
\begin{aligned}
S^{\mu_2\nu_2;\rho\omega}_{\chi_{c2}} &= \frac{-i}{P^2-M^2_{\chi_{c2}}+iM_{\chi_{c2}}\Gamma_{\chi_{c2}}}\{\frac{1}{2}(g^{\mu_2\rho}\frac{P^{\nu_2}P^\omega}{M^2_{\chi_2}}+g^{\nu_2\omega}\frac{P^{\mu_2}P^\rho}{M^2_{\chi_{c2}}}+g^{\mu_2\omega}\frac{P^{\nu_2}P^\rho}{M^2_{\chi_{c2}}}+g^{\nu_2\rho}\frac{P^{\mu_2}P^\omega}{M^2_{\chi_{c2}}})\\
&\quad +\frac{1}{2}(g^{\mu_2\rho}g^{\nu_2\omega}+g^{\mu_2\omega}g^{\nu_2\rho}-g^{\mu_2\nu_2}g^{\rho\omega})+\frac{2}{3}(\frac{1}{2}g^{\mu_2\nu_2}-\frac{P^{\mu_2}P^{\nu_2}}{M^2_{\chi_{c2}}})(\frac{1}{2}g^{\rho\omega}-\frac{P^\rho P^\omega}{M^2_{\chi_{c2}}})\}.
\end{aligned}
\tag{8}
$$

With Eqs. (4,5,8), the corresponding amplitudes for the diagrams in the right panel of Fig.1 can be written down. Their interferences with Born diagrams can be calculated directly and we use the FeynCalc [24] to do the analysis calculation and LoopTools [25] for the numerical calculation.

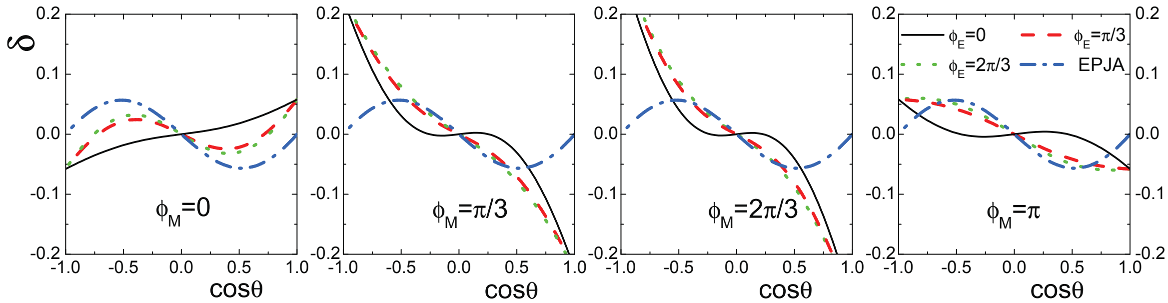

Figure 2: The cosθ dependence of δ at $\sqrt{s} = M_{\chi_{c2}}$ by χ_{c2} contributions to TPE effects. The black solid, red dashed and green dotted curves are corresponding to $\phi_E = 0, \pi/3$ and $2/3\pi$, the blue dashed-dotted curves named as EPJA are explained in the text.

4 Results

Since only χ_{c2} gives the contributions, we limit the discussion in $\sqrt{s} \sim M_{\chi_{c2}}$. To show the TPE contributions, we define

$$
\begin{aligned}
\delta &\equiv \frac{d\sigma^{(1)}/d\Omega}{d\sigma^{(0)}/d\Omega}, \\
A^{[\theta_0-\theta_1]} &\equiv \frac{2\pi\int_{\theta_0}^{\theta_1}(d\sigma^{(0)}+d\sigma^{(1)})/d\Omega sin\theta d\theta - 2\pi\int_{\pi-\theta_1}^{\pi-\theta_0}(d\sigma^{(0)}+d\sigma^{(1)})/d\Omega sin\theta d\theta}{2\pi\int_{\theta_0}^{\theta_1}(d\sigma^{(0)}+d\sigma^{(1)})/d\Omega sin\theta d\theta + 2\pi\int_{\pi-\theta_1}^{\pi-\theta_0}(d\sigma^{(0)}+d\sigma^{(1)})/d\Omega sin\theta d\theta} \\
&= \frac{\int_{\theta_0}^{\theta_1} d\sigma^{(1)}/d\Omega sin\theta d\theta}{\int_{\theta_0}^{\theta_1} d\sigma^{(0)}/d\Omega sin\theta d\theta}, \qquad (9)
\end{aligned}
$$

with $d\sigma^{(1)}/d\Omega$ the unpolarized differential cross section from the interference of TPE diagrams and Born diagrams. By the crossing symmetry and Lorentz invariance, we have the relation for the amplitudes $M(e^+(k_2)e^-(k_1) \to p(p_2)\bar{p}(p_1)) = M(p(-p_1)\bar{p}(-p_2) \to e^+(-k_1)e^-(-k_2)) = M(p(p_1)\bar{p}(p_2) \to e^+(k_1)e^-(k_2))$, which means the ratios of cross sections $\delta, A^{[\theta_0-\theta_1]}$ in $e^+e^- \to p\bar{p}$ are the same as those in $p\bar{p} \to e^+e^-$.

The θ and ϕ_M dependence of δ at $\sqrt{s} = M_{\chi_{c2}}$ are presented in Fig.2 and Fig.3. The results show the TPE contributions to δ by χ_{c2} are almost independent on ϕ_E, especially at small θ, while are strongly dependent on θ and ϕ_M. The corrections δ are odd functions of $\cos\theta$, which is a general property of 2γ annihilation effects. The most interesting property of Fig.3 is that the absolute corrections $|\delta|$ are larger than 10% at small θ ($\theta \leq \pi/10$) for almost all ϕ_M.

To compare with the measurement precision of coming PANDA detector, we present the corresponding δ used by the PANDA simulations [26] as the curves labeled EPJA in Fig.2. By the definition of our δ and TPE contribution Eq.(14) of Ref. [26], we have

$$
\delta = \frac{2\sqrt{\tau(\tau+1)}(G_E/\tau - G_M)F_3 cos(\theta) sin^2(\theta)}{G_M^2(1+cos^2(\theta)) + (G_E^2/\tau)sin^2(\theta)}, \qquad (10)
$$

with $\tau = s/4M_N^2$ and F_3 defined by Eq.(14) of Ref. [26]. The curve of δ named as EPJA in Fig.2 is corresponding to the case $F_3/G_M = 5\%$ assuming $G_E = G_M$. The results in Fig.2 show that the realistic

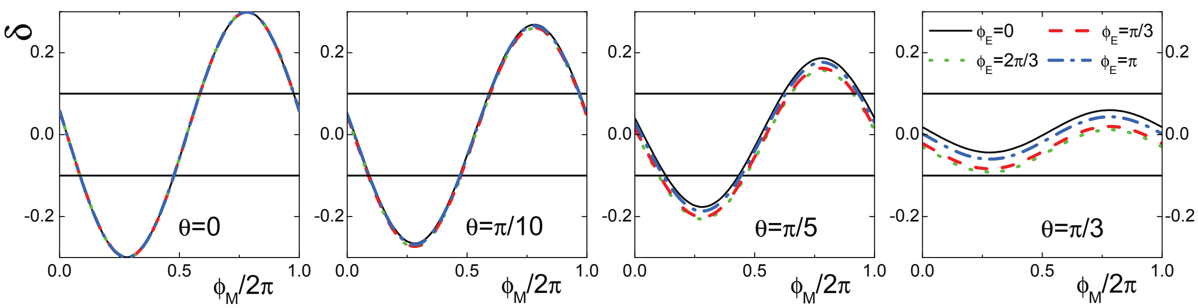

Figure 3: The ϕ_M dependence of δ at $\sqrt{s} = M_{\chi_{c2}}$ by χ_{c2} contributions to TPE effects. The black solid, red dashed, green dotted and blue dashed-dotted curves are corresponding to $\phi_E = 0, \pi/3, 2/3\pi$ and π.

δ in the small θ ($|cos\theta| > 0.8$) are much larger than δ(EPJA) for most ϕ_M. In the region where PANDA detector works, the realistic δ are larger than δ(EPJA) in the region $0.5 < |cos\theta| < 0.8$ and comparable with δ(EPJA) in the region $|cos\theta| < 0.5$ for some ϕ_M, for example $\phi_M = 1/3\pi, 2/3\pi$.

The full results show that the TPE contributions to δ from χ_{c2} are much larger than the usual TPE effects from non-resonance contributions. The latter are usually less than 1% at small θ [6, 7] and is a challenge to be observed by PANDA [7], while the former are comparable with the measurement precision of PANDA at $\sqrt{s} \sim M_{\chi_{c2}}$. This suggests that the coming PANDA experiment may detect the direct TPE effects at $\sqrt{s} \sim M_{\chi_{c2}} \pm 0.01$ GeV. And outside of this region, the TPE contributions from χ_2 are as small as 1% at the small θ ($\theta < \pi/10$) and the corrections to the measurements of $G_{M,E}$ will be very small [26].

Fig.4 displays the curves of forward-backward asymmetry $A^{[\theta_0-\theta_1]}$ vs. ϕ_M at $\sqrt{s} = M_{\chi_{c2}}, M_{\chi_{c2}} \pm 0.001$ GeV with $\phi_E = 0$ as an example. The left panel of Fig.4 shows that the forward-backward asymmetry with $\theta_0 = \pi/5, \theta_1 = \pi/2$ is larger than 2% for almost all ϕ_M when combining the three $\sqrt{s}$ points. The right panel of Fig.4 shows that the forward-backward asymmetry with smaller $\theta_1 = \pi/3$ is much enhanced. Fig.5 displays the $\phi_{E,M}$ dependence of $A^{[\pi/5-\pi/3]}$ and $A^{[\pi/5-\pi/2]}$ in contour form, which shows the properties of forward-backward asymmetry in the parameter space more clearly. By the simulation of PANDA detector [26], the reconstructed number of counts at $s = 12.9$ GeV^2 ($\sim M^2_{\chi_{c2}}$) is about 10^3 for $|cos\theta| < 0.8$ (corresponding to $\theta > 1/5\pi$). The left panel of Fig.5 shows that the number of asymmetry events for $\theta \subseteq [\pi/5 - \pi/2]$ at $\sqrt{s} \sim M_{\chi_{c2}}$ is larger than 20 for almost all $\phi_{E,M}$ and larger than 40 most $\phi_{E,M}$.

To show the property of asymmetry events number, we define the ratio $\bar{R}$ as

$$\bar{R} \equiv \frac{\int_{\theta_0}^{\theta_1} d\sigma^{(1)}/d\Omega sin\theta d\theta}{\int_{\theta_0}^{\pi/2} d\sigma^{(1)}/d\Omega sin\theta d\theta}. \tag{11}$$

The angle θ_1 dependence of ratio $\bar{R}$ at $\sqrt{s} = M_{\chi_{c2}}$ with $\theta_0 = \pi/5$ is presented in Fig.6 which shows two interesting properties: (1) $\bar{R}$ is almost independent on $\phi_{E,M}$ except for at very small ϕ_M. The special behavior of $\bar{R}$ at very small ϕ_M is corresponding to the property of δ at $\phi_M = 0$ in Fig.2, which is not monotonic function of $cos\theta$ in the region $\theta \subseteq [\pi/5, \pi/2]$; (2) $\bar{R}$ reaches about 80% for $\theta_1 = \pi/3$ and 90% for $\theta_1 = 2\pi/5$. These two properties indicate that whatever $\phi_{E,M}$ are, for experiments, most of the forward-backward asymmetry events lie in $\theta \subseteq [\pi/5, \pi/3]/[2\pi/3, 4\pi/5]$ when the detector works in the region $|cos\theta| < 0.8$.

In conclusion, our calculation shows the resonance χ_{c2} contributions to TPE effects may give large

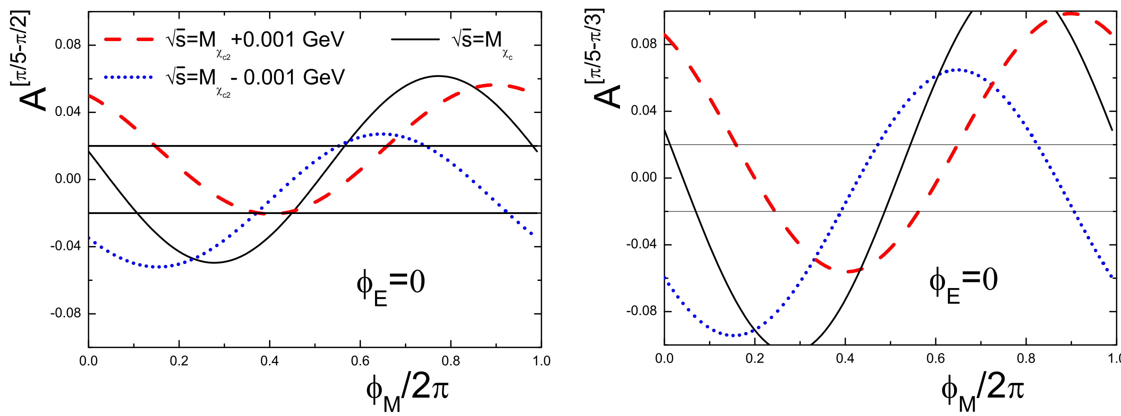

Figure 4: The ϕ_M dependence of forward-backward asymmetry at $\sqrt{s} \sim M_{\chi_{c2}}$ with $\phi_E = 0$. The red dashed, black solid and blue dotted curves are corresponding to $\sqrt{s} = M_{\chi_{c2}} + 0.001$ GeV, $M_{\chi_{c2}}$ and $M_{\chi_{c2}} - 0.001$ GeV.

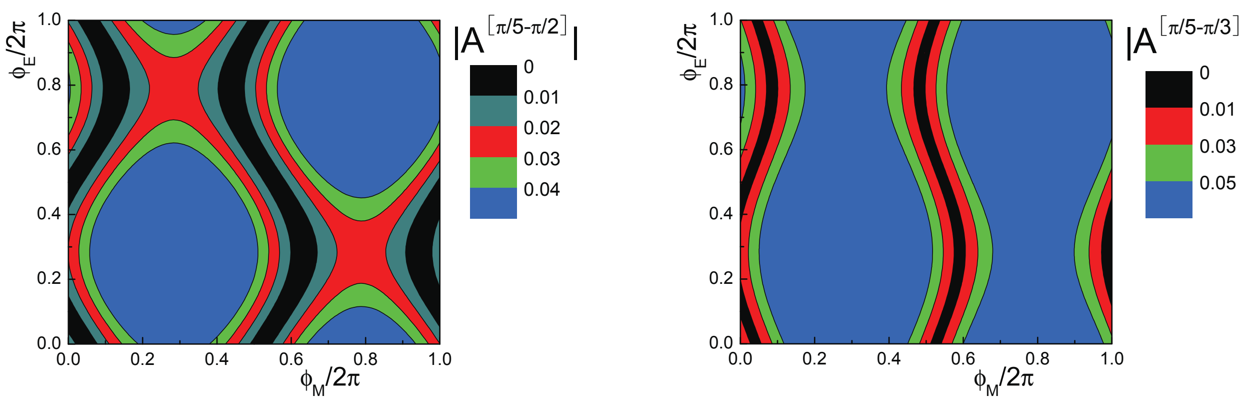

Figure 5: The $\phi_{M,E}$ dependence of absolute forward-backward asymmetry at $\sqrt{s} = M_{\chi_{c2}}$ in contour form.

corrections in $e^+e^- \leftrightarrow p\overline{p}$ when $\sqrt{s} \sim M_{\chi_{c2}}$. The results suggest that the coming experiment PANDA may detect the direct TPE effects in small scattering angle region such as $\theta \subseteq [\pi/5, \pi/3]$ at $\sqrt{s} \sim M_{\chi_{c2}}$. For lower energies around 2.3 GeV, the contributions from resonances of light flavor quarks should also play similar important role in $e^+e^- \leftrightarrow p\bar{p}$.

5 Acknowledgment

This work is supported by the National Natural Science Foundation of China under grants Nos. 10805009 and 11035006.

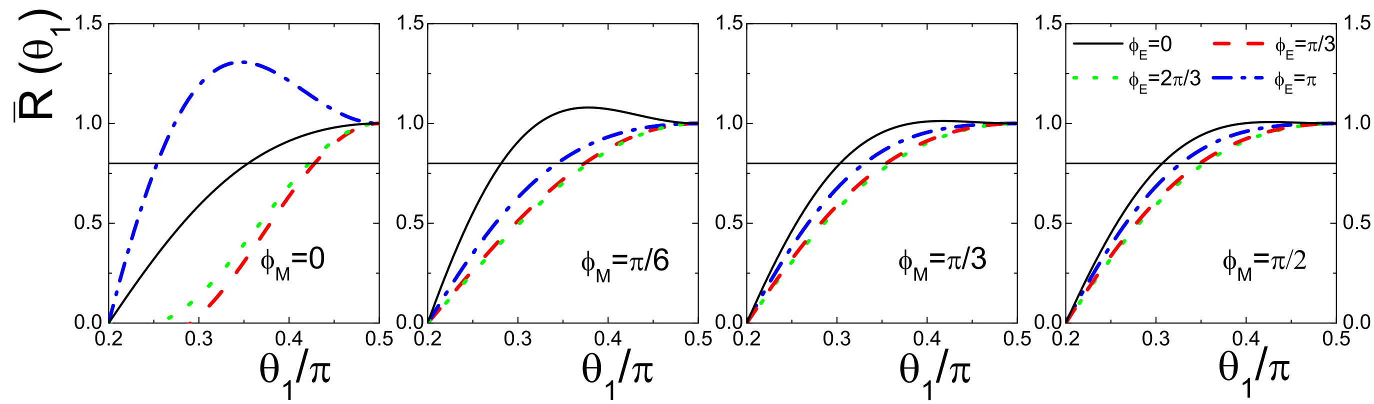

Figure 6: The θ_1 dependence of R at $\sqrt{s} = M_{\chi_{c2}}$ with $\theta_0 = \pi/5$. The black solid, red dashed, green dotted and blue dashed-dotted curves are corresponding to $\phi_E = 0, \pi/3, 2/3\pi$ and π.

References

[1] R.C. Walker et al., Phys. Rev. D 49 (1994) 5671; L. Andivahis et al., Phys. Rev. D 50 (1994) 5491; M.K. Jones et al., Phys. Rev. Lett. 84 (2000) 1398; O. Gayou et al., Phys. Rev. Lett. 88 (2002) 092301.

[2] P.G. Blunden, W. Melnitchouk, J.A. Tjon, Phys. Rev. Lett. 91 (2003) 142304; S. Kondratyuk, P.G. Blunden, W. Melnitchouk, J.A. Tjon, Phys. Rev. Lett. 95 (2005) 172503.

[3] Y.C. Chen, A.V. Afanasev, S.J. Brodsky, C.E. Carlson, M. Vanderhaeghen, Phys. Rev. Lett93 (2004) 122301.

[4] Dmitry Borisyuk, Alexander Kobushkin, Phys. Rev. C 78 (2008) 025208.

[5] Dmitry Borisyuk, Alexander Kobushkin, Phys. Rev. D 79 (2009) 034001; Nikolai Kivel, Marc Vanderhaeghen, Phys. Rev. Lett.103 (2009) 092004.

[6] D.Y. Chen, H.Q. Zhou, Y.B. Dong, Phys. Rev. C 78 (2008) 045208; Hai Qing Zhou, Dian Yong Chen, Yu Bing Dong, Phys. Lett. B 675 (2009) 305.

[7] Julia Guttmann, Nikolai Kivel, Marc Vanderhaeghen, Phys. Rev. D 83 (2011) 094021.

[8] Pierre A.M. Guichon, M. Vanderhaeghen, Phys. Rev. Lett.91 (2003) 142303;

[9] Michail P. Rekalo, Egle Tomasi-Gustafsson, Eur. Phys. J. A22 (2004) 331; E. Tomasi-Gustafsson, G.I. Gakh, Phys. Rev. C 72 (2005) 015209.

[10] J. Arrington, Phys. Rev. C 69 (2004) 032201; J. Arrington, Phys. Rev. C 71(2005)015202; J. Arrington, W. Melnitchouk, J. A. Tjon, Phys. Rev. C 76 (2007) 035205.

[11] Yu-Chun Chen, Chung-Wen Kao, Shin-Nan Yang, Phys. Lett. B 652 (2007) 269.

[12] M. A. Belushkin, H.-W. Hammer, U.-G. Meissner, Phys. Lett. B 658 (2008) 138.

[13] G.I. Gakh, E. Tomasi-Gustafsson, Nucl. Phys. A 771 (2006) 169; E. Tomasi-Gustafsson, E.A. Kuraev, S. Bakmaev, S. Pacetti, Phys. Lett. B 659 (2008) 197.

[14] Carl E. Carlson, Marc Vanderhaeghen, Ann. Rev. Nucl. Part. Sci. 57 (2007) 171; J. Arrington, P. G. Blunden, W. Melnitchouk, Prog. Part. Nucl. Phys. 66 (2011) 782.

[15] J. Arrington, D. M. Nikolenko et al., nucl-ex/0408020; D.M. Nikolenko et al., Phys. Atom. Nucl. 73 (2010) 1322; D.M. Nikolenko et al., PoS ICHEP 2010 (2010) 164.

[16] W. Brooks et al., Jefferson lab experiment E07-005.

[17] M. Kohl, AIP Conf. Proc. 1160 (2009) 19; M. Kohl, AIP Conf.Proc.1374(2011)527.

[18] PANDA Collaboration, arXiv: 0903.3905; M. Sudol et al., Eur. Phys. J. A 44 (2010) 373.

[19] T. Barnes, X. Li, W. Roberts, Phys. Rev. D 77 (2008) 056001.

[20] Where q is corrected as $(\sqrt{s}, 0, 0, 0)$ in c.m frame comparing with [19].

[21] Johann H. Kuhn, Jean Kaplan, El Ghali Oudrhiri Safiani, Nucl. Phys. B 157 (1979) 125; D. Ebert, R.N. Faustov, V. O. Galkin, Mod. Phys. Lett. A 18 (2003) 601.
[22] K Nakamura et al (Particle Data Group)., J. Phys. G 37 (2010) 075021.
[23] Shi-Zhong Huang, Peng-Fei Zhang, Tu-Nan Ruan, Yu-Can Zhu, Zhi-Peng Zheng, Eur. Phys. J. C 42 (2005) 375.
[24] R. Mertig, M. Bohm, A. Denner, Comput. Phys. Commun. 64 (1991) 345.
[25] T. Hahn, M. Perez-Victoria, Comput. Phys. Commun. 118 (1999) 153.
[26] M. Sudol et al., Eur. Phys. J. A 44 (2010) 373.